

Height from Gradient Using Surface Curvature and Area Constraints

Tiangong Wei and Reinhard Klette

CITR, Department of Computer Science, Tamaki Campus
The University of Auckland, Private Bag 92019, Auckland, New Zealand
{tiangong, r.klette}@tcs.auckland.ac.nz

Abstract

This paper presents a regularization method for surface reconstruction from noisy gradient vector fields. The algorithm takes as its input a discrete gradient vector field, obtained by applying a Shape from Shading or Photometric Stereo method. To derive this algorithm, we combine the integrability constraint and the surface curvature and area constraints into a single functional, which is then minimized. Therefore, value changes in the height or depth map will be more regular. To solve the minimization problem, we employ the Fourier transform theory rather than the Variational Principle. The Fourier transform of the unknown surface is expressed as a function of the given gradient's Fourier transforms. The relative depth values can be obtained by an inverse Fourier Transform and by choosing associated weighting parameters. The method is evaluated on gradient data delivered by a shape-from-shading algorithm.

1. Introduction

Recovering 3D surface shape of objects, classified as shape-from-X techniques, is a classic and important research areas of computer vision. Many of the existing methods, e.g. shape from shading (SFS) and photometric stereo method (PSM), normally provide gradient values (i.e the discrete gradient vector field) or surface normals for a discrete set of visible points on object surfaces. However, in order to achieve the relative height or depth values of the surface, these discrete surface gradients must to be integrated by using gradient integration techniques. In practice, the gradient vector fields are normally contaminated by noise because each captured image is influenced by the presence of camera noise and further measurement errors.

In this paper, we suppose that the surface function $Z(x, y)$ of a scene object is formed by an orthographic (parallel) projection of the surface into the xy -image plane, and defined in the image plane over a compact

region Ω . The gradient values of this surface at discrete points $(x, y) \in \Omega$

$$p(x, y) = \frac{\partial Z(x, y)}{\partial x} = Z_x$$

and

$$q(x, y) = \frac{\partial Z(x, y)}{\partial y} = Z_y$$

are only available as input data and contaminated by noise, for instance, in the form of a given imperfect *needle diagram*.

Essentially there are two main classes of integration techniques for finding surface height $Z(x, y)$ from discrete gradients $p(x, y)$ and $q(x, y)$: *local integration techniques* and *global integration techniques* (for a review, see Klette and Schlüns [7]). Local integration methods such as two-point method[1] and eight-point[3] are conceptually simple. The surface height can be recovered by considering the surface normal vectors at the two or eight adjacent points of a given point, computing the average tangent through the given point, and interpolating the height and the surface normals. Wu and Li [12] proposed a method based on the following curve integrals:

$$Z(x, y) = Z(x_0, y_0) + \int_{\gamma} p(x, y)dx + q(x, y)dy, \quad (1)$$

where γ is an arbitrarily specified integration path from (x_0, y_0) to $(x, y) \in \Omega$. Starting with initial height values, the methods propagate height values according to a local approximation rule (e.g., based on the 4-neighborhood) using the given gradient data. Such a calculation of relative height values can be repeated by using different scan algorithms. Finally, resulting height values can be determined by averaging operations. However, initial height values have to be provided. The locality of the computations propagates errors along the integration path, i.e. this approach strongly depends on data accuracy. Therefore, local

integration techniques perform badly when the data are noisy.

The equations linking the surface height and gradients are $p = Z_x$ and $q = Z_y$, so global integration techniques (Horn and Brooks [4], Frankot and Chellappa [2], Horn [5], Wei and Klette [10, 11]) are based on minimizing the following functional (cost function):

$$W = \iint_{\Omega} [|Z_x - p|^2 + |Z_y - q|^2] dx dy. \quad (2)$$

Comparing with the local methods, the Frankot-Chellappa algorithm, based on the results of the paper [2] and presented in Klette et. al [8], leads to better results for the task of calculating surface height from gradients. At each iteration of the algorithm, the non-integrable surface is converted into the integrable surface by orthogonal projection in the frequency domain. Nevertheless, the errors of the algorithm are high for the imperfect estimate of the surface gradient or noisy gradient vector fields. Also, the algorithm is very sensitive to the abrupt changes in orientation, i.e. there are large errors at the object boundary. Noakes, Kozer and Klette [9] proposed a Lawn-Mowing algorithm for enforcing the integrability condition of a given non-integrable vector field, but there are no experimental results reported for real images.

The organization of the rest of the paper is as follows. In Section 2 we present our new algorithm for height from gradient. The experimental results with noise added synthetic data, and with real data are shown in Section 3. Finally, conclusions are given in Section 4

2. Height from Gradient

In the following, we apply the Fourier transform theory to derive a new algorithm for solving the height from gradients. In order to improve the accuracy and robustness, and to strengthen the relation between the estimated surface and the original image, the functional to be minimized is as follows:

$$\begin{aligned} W = & \iint_{\Omega} [|Z_x - p|^2 + |Z_y - q|^2] dx dy \\ & + \lambda \iint_{\Omega} (|Z_x|^2 + |Z_y|^2) dx dy \\ & + \mu \iint_{\Omega} (|Z_{xx}|^2 + 2|Z_{xy}|^2 + |Z_{yy}|^2) dx dy \end{aligned} \quad (3)$$

where the subscripts indicate partial derivatives. In the above cost function, the second term of the right-hand is a small deflection approximation of the surface area, and the third term is a small deflection approximation of the surface curvature (i.e it is a measure of

quadratic variation in the surface slopes). The non-negative regularization parameters λ and μ establish a trade-off between the constraints, i.e it is used to adjust the weighting between them. The above new cost function reflects the relations among the surface height $Z(x, y)$, surface gradient $p(x, y)$ and $q(x, y)$ more effectively, and make the best use of the information provided by the surface gradient.

The following objective is to solve the unknown $Z(x, y)$ subject to an optimization process which minimizes the cost function W . To find the minimum of the functional W , most of the algorithms used in computer vision use calculus of variations to produce the Euler-Lagrange equations. Then a discrete version of the Euler-Lagrange equations can be obtained by discretizing or differentiating. Instead of using variational calculus, we use the Fourier transform theory. Suppose that the Fourier transform of the surface function $Z(x, y)$ is

$$Z_F(u, v) = \iint_{\Omega} Z(x, y) e^{-j(ux+vy)} dx dy, \quad (4)$$

and the inverse Fourier transform is

$$Z(x, y) = \frac{1}{2\pi} \iint_{\Omega} Z_F(u, v) e^{j(ux+vy)} du dv, \quad (5)$$

where j is the imaginary unit. According to the differentiation properties of the Fourier transform, we have

$$\begin{aligned} Z_x(x, y) & \leftrightarrow juZ_F(u, v), \\ Z_y(x, y) & \leftrightarrow jvZ_F(u, v), \\ Z_{xx}(x, y) & \leftrightarrow -u^2Z_F(u, v), \\ Z_{yy}(x, y) & \leftrightarrow -v^2Z_F(u, v), \\ Z_{xy}(x, y) & \leftrightarrow -uvZ_F(u, v). \end{aligned}$$

Let $\bar{P}(u, v)$ and $\bar{Q}(u, v)$ be the Fourier transforms of $p(x, y)$ and $q(x, y)$, respectively. Taking the Fourier transform in (3) and using the above differentiation properties and the following Parseval's formula

$$\iint_{\Omega} |Z(x, y)|^2 dx dy = \frac{1}{2\pi} \iint_{\Omega} |Z_F(u, v)|^2 du dv,$$

we obtain

$$\begin{aligned} & \frac{1}{2\pi} \iint_{\Omega} [|juZ_F(u, v) - \bar{P}(u, v)|^2 + \\ & + |jvZ_F(u, v) - \bar{Q}(u, v)|^2] du dv + \\ & + \frac{\lambda}{2\pi} \iint_{\Omega} [|juZ_F(u, v)|^2 + |jvZ_F(u, v)|^2] du dv \\ & + \frac{\mu}{2\pi} \iint_{\Omega} [|-u^2Z_F(u, v)|^2 + 2|-uvZ_F(u, v)|^2 + \\ & + |-v^2Z_F(u, v)|^2] du dv \rightarrow \text{minimum}, \end{aligned}$$

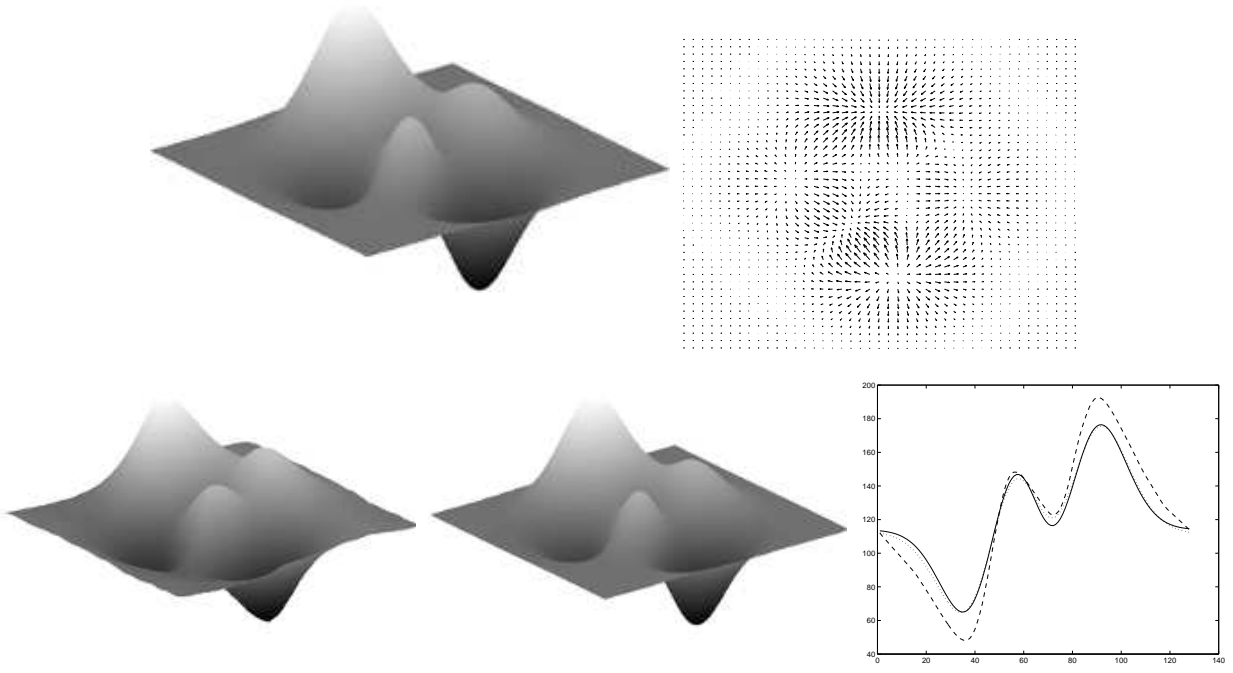


Figure 1: Results of a synthetic image. (a) Intensity image. (b) Gradient vector field. (c) Reconstructed surface with $\lambda = 0, \mu = 0$. (d) Reconstructed surface with $\lambda = 0.1, \mu = 10$. (e) $z - y$ plane sliced at $x=64$, where solid line for real surface, dashed line for $\lambda = 0, \mu = 0$, and dotted line for $\lambda = 0.1, \mu = 10$

The left side of the above expression can be expanded as

$$\begin{aligned} & \frac{1}{2\pi} \iint_{\Omega} [u^2 Z_F Z_F^* - ju Z_F P^* + ju Z_F^* P + P P^* \\ & + v^2 Z_F Z_F^* - jv Z_F Q^* + jv Z_F^* Q + Q Q^*] dudv \\ & + \frac{\lambda}{2\pi} \iint_{\Omega} (u^2 + v^2) Z_F Z_F^* dudv \\ & + \frac{\mu}{2\pi} \iint_{\Omega} (u^4 + 2u^2 v^2 + v^4) Z_F Z_F^* dudv, \end{aligned}$$

where $*$ denotes the conjugate. Differentiating the above expression with respect to Z_F and Z_F^* , we can deduce the following minimal conditions for the cost function (3)

$$C_{uv} Z_F + juP + jvQ = 0,$$

$$C_{uv} Z_F^* - juP^* - jvQ^* = 0.$$

where $C_{uv} = (1 + \lambda)(u^2 + v^2) + \mu(u^2 + v^2)^2$. Adding the above two equations together, then subtracting the first one from the second one, this results in the following equations

$$C_{uv}(Z_F + Z_F^*) + ju(P - P^*) + jv(Q - Q^*) = 0,$$

and

$$C_{uv}(Z_F - Z_F^*) + ju(P + P^*) + jv(Q + Q^*) = 0.$$

Solving the above equations except for $(u, v) \neq (0, 0)$, we obtain

$$Z_F(u, v) = \frac{-juP(u, v) - jvQ(u, v)}{(1 + \lambda)(u^2 + v^2) + \mu(u^2 + v^2)^2} \quad (6)$$

where $(u, v) \neq (0, 0)$. Therefore, the Fourier transform of the surface is expressed as a function of the Fourier transforms of given gradients $p(x, y)$ and $q(x, y)$. The main result is summarized in the following theorem.

Theorem 1 *The cost function (3) is minimized by taking the Fourier transform of surface $Z(x, y)$ as in the formula (6).*

The Frankot-Chellappa algorithm [2] as formulated in [8], is a special case when parameter $\lambda = 0$ and $\mu = 0$ in (3). Therefore, let $\lambda = 0$ and $\mu = 0$ in (6), we obtain that the objective functional (2) is minimized by taking the Fourier transform of the surface $Z(x, y)$ as

$$Z_F(u, v) = \frac{-1}{u^2 + v^2} [juP(u, v) + jvQ(u, v)], \quad (7)$$

Algorithm 1 New algorithm for height from gradient

```
1: input gradients  $p(x, y), q(x, y), \lambda$  and  $\mu$ 
2: for  $0 \leq x, y \leq N - 1$  do
3:   if ( $|p(x, y)| < max_{pq}$  &  $|q(x, y)| < max_{pq}$ ) then
4:      $P1(x, y) = p(x, y); P2(x, y) = 0;$ 
5:      $Q1(x, y) = q(x, y); Q2(x, y) = 0;$ 
6:   else
7:      $P1(x, y) = 0; P2(x, y) = 0;$ 
8:      $Q1(x, y) = 0; Q2(x, y) = 0;$ 
9:   end if
10: end for
11: Calculate the Fourier transforms of  $P1(x, y)$  and
 $P2(x, y)$ :  $P1(u, v), P2(u, v);$ 
12: Calculate the Fourier transforms of  $Q1(x, y)$  and
 $Q2(x, y)$ :  $Q1(u, v), Q2(u, v);$ 
13: for  $0 \leq u, v \leq N - 1$  do
14:   if ( $u \neq 0$  &  $v \neq 0$ ) then
15:      $\Lambda = (1 + \lambda)(u^2 + v^2) + \mu(u^2 + v^2)^2;$ 
16:      $\Delta 1 = uP2(u, v) + vQ2(u, v);$ 
17:      $\Delta 2 = -uP1(u, v) - vQ1(u, v);$ 
18:      $H1(u, v) = \Delta 1 / \Lambda;$ 
19:      $H2(u, v) = \Delta 2 / \Lambda;$ 
20:   else
21:      $H1(0, 0) = \text{average height}; H2(0, 0) = 0;$ 
22:   end if
23: end for
24: Calculate the inverse Fourier transforms of  $H1(u, v)$ 
and  $H2(u, v)$ :  $H1(x, y), H2(x, y);$ 
25: for  $0 \leq x, y \leq N - 1$  do
26:    $Z(x, y) = H1(x, y);$ 
27: end for
```

where $(u, v) \neq (0, 0)$. The formula (7) can also be derived using the above process directly. If so, the process deriving (7) is much simpler than the one used by Frankot-Chellappa in [2]. On the other hand, our new algorithm is capable of dealing with additional constraints.

The Algorithm 1 shows our proposed method for the task of calculating depth from gradients, which use the transformation as specified in Theorem 1 after having the Fourier transforms of the given gradient field. Then an inverse Fourier transform leads to the desired depth map, which allows us to reconstruct object surfaces in 3D space within a subsequent computation step of a general back projection approach.

If the gradient vectors of any length are used as input to the algorithm, then the reconstructed surface is distorted. To avoid this, the value $max_{pq} = 4$ was used in the experiments that are described in the next section.

3. Experimental Results

For an analysis of depth from noisy gradient vector fields, the algorithm described earlier was implemented with one synthetic image and two real images. The discrete gradients were generated using a shape from shading algorithm proposed by Ikeuchi and Horn [6]. The Gaussian noise (with a mean set zero and a standard deviation set to 0.01) was subsequently added to the gradient vector fields obtained from the corresponding surfaces.

Figure 1 shows the reconstructed surfaces for a synthetic image with $\lambda = 0, \mu = 0$ and $\lambda = 0.1, \mu = 10$, and the $z - y$ plane sliced at $x = 64$, where the solid line represents the real surface, dashed line represents the reconstructed surface with $\lambda = 0, \mu = 0$, and dotted line for $\lambda = 0.1, \mu = 10$.

Figure 2 illustrates the reconstructed surfaces for a torus object with $\lambda = 0, \mu = 0$ and $\lambda = 0.1, \mu = 15$ and the $z - y$ plane sliced at $x = 100$, where the solid line represents the object surface, dashed line represents the reconstructed surface with $\lambda = 0, \mu = 0$, and dotted line for $\lambda = 0.1, \mu = 15$.

Figure 3 shows the reconstructed surfaces for a vase object with $\lambda = 0, \mu = 0$ and $\lambda = 0.1, \mu = 10$ and the $z - y$ plane sliced at $x = 100$, where the solid line represents the object surface, dashed line represents the reconstructed surface with $\lambda = 0, \mu = 0$, and dotted line for $\lambda = 0.1, \mu = 10$.

Our evaluation is also done by providing quantitative measures on how well the reconstructed surface matches the original by looking at the Mean Square Error (MSE). The errors for the three images are shown in Table 1.

Surfaces	Parameters	MSE
Peaks	$\lambda = 0, \mu = 0$	15.5
Peaks	$\lambda = 0.1, \mu = 10$	5.8
Torus	$\lambda = 0, \mu = 0$	32.5
Torus	$\lambda = 0.1, \mu = 15$	2.7
Vase	$\lambda = 0, \mu = 0$	22.4
Vase	$\lambda = 0.1, \mu = 10$	4.0

Table 1: Mean Square Error for the reconstructed surfaces

From the reconstructed surfaces, we can see that the depth recovery is improved by choosing corresponding regularization parameters. The mean square errors are also much smaller. Therefore, the experimental results showed the proposed algorithm is a robust method for surface height recovery from surface gradients.

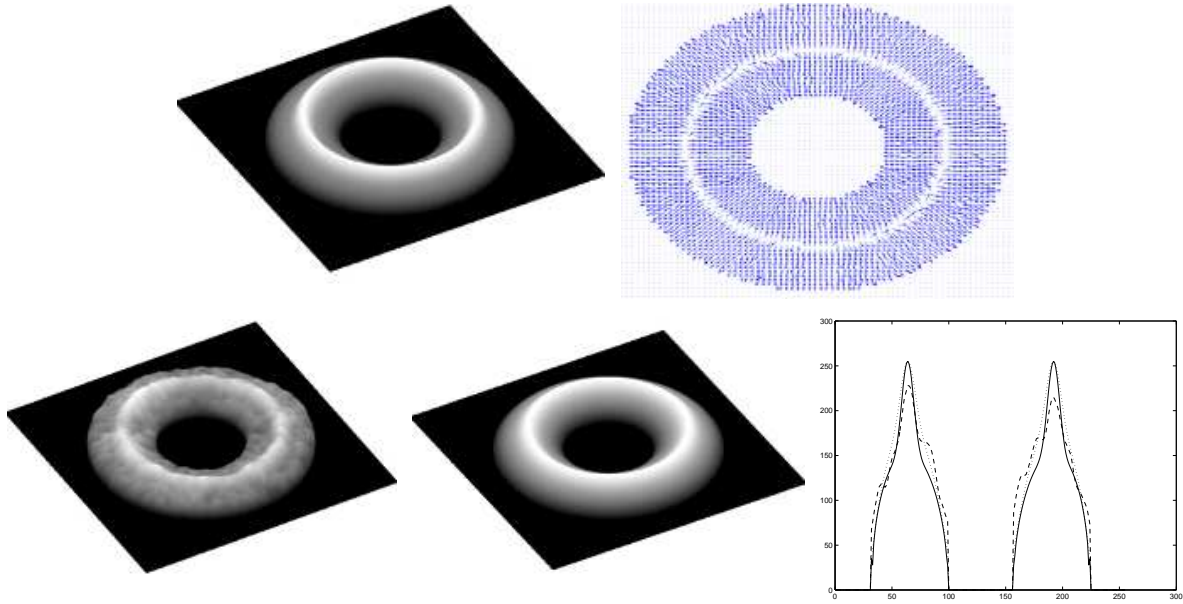


Figure 2: Results of a torus object. (a) Intensity image. (b) Gradient vector field. (c) Reconstructed surface with $\lambda = 0, \mu = 0$. (d) Reconstructed surface with $\lambda = 0.1, \mu = 15$. (e) $z - y$ plane sliced at $x=100$, where solid line for real surface, dashed line for $\lambda = 0, \mu = 0$, and dotted line for $\lambda = 0.1, \mu = 15$

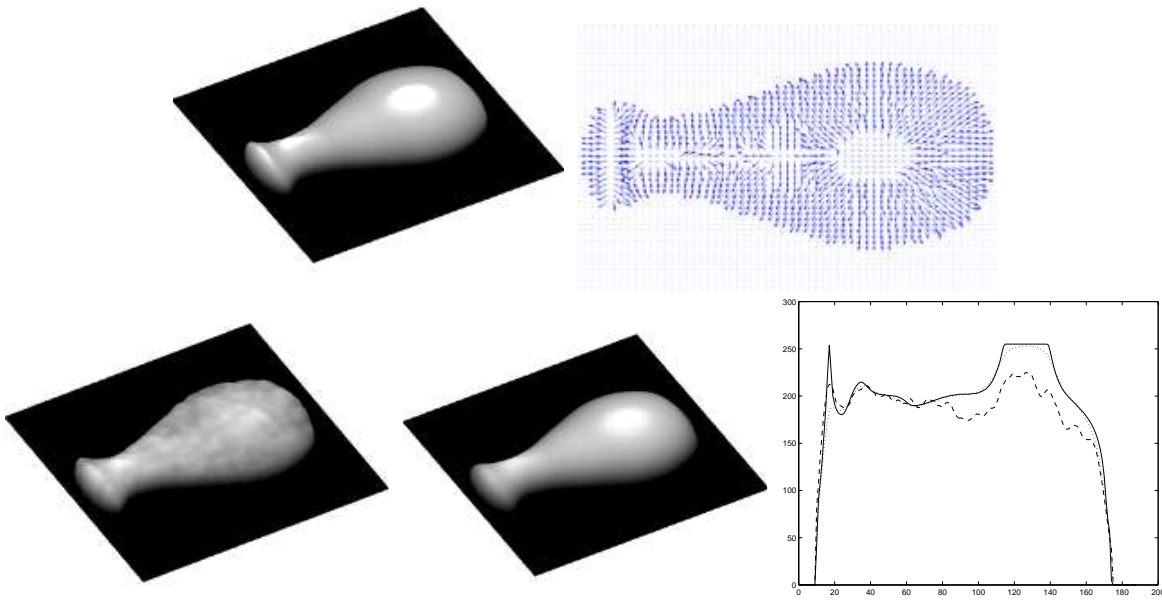


Figure 3: Results of a vase object. (a) Intensity image. (b) Gradient vector field. (c) Reconstructed surface with $\lambda = 0, \mu = 0$. (d) Reconstructed surface with $\lambda = 0.1, \mu = 10$. (e) $z - y$ plane sliced at $x=100$, where solid line for real surface, dashed line for $\lambda = 0, \mu = 0$, and dotted line for $\lambda = 0.1, \mu = 10$

4. Conclusions

We designed a new algorithm for depth from gradient vector fields. The new cost function reflects the

relations among surface height and surface gradients more effectively. The new algorithm is capable of deal-

ing with additional constraints. The choose of regularization parameters heavily affects the surface reconstruction from noisy gradients. The relation between the parameters and noise should be the future research topic. The appropriateness of the approach has been illustrated through experiments using synthetic image and real objects.

References

- [1] N. E. Coleman, Jr. and R. Jain: Obtaining 3-dimensional shape of textured and specular surfaces using four-source photometry. *CGIP*, **18** (1982) 439–451.
- [2] R. T. Frankot and R. Chellappa: A method for enforcing integrability in shape from shading algorithms. *IEEE Transactions on pattern Analysis and Machine Intelligence*, **10** (1988) 439–451.
- [3] G. Healey and R. Jain: Depth recovery from surface normals. *ICPR '84*, Montreal, Canada, Jul. 30 – Aug. 2 **2** (1984) 894-896.
- [4] B. K. P. Horn and M. J. Brooks: The variational approach to shape from shading. *Computer Vision, Graphics, and Image Processing*, **33** (1986) 174–208.
- [5] B. K. P. Horn: Height and gradient from shading. *International Journal of Computer Vision*, **5** (1990) 37–75.
- [6] K. Ikeuchi and B. K. P. Horn: Numerical shape from shading and occluding boundaries. *Artificial Intelligence*, **17** (1981) 141–184.
- [7] R. Klette and K. Schlüns: Height data from gradient fields. *Proceedings of SPIE (the international Society for Optical Engineering) on Machine Vision Applications, Architectures, and Systems Integration*, Boston, Massachusetts, USA. **2908** (1996) 204–215.
- [8] R. Klette, K. Schlüns and A. Koschan: *Computer Vision - Three-dimensional Data from Images*. Springer, Singapore, 1998.
- [9] L. Noakes, R. Kozera and R. Klette: The Lawn-Mowing algorithm for noisy gradient vector fields. *Proceedings of SPIE (the international Society for Optical Engineering), Vision Geometry VIII*, Denver, Colorado, USA. **3811** (1999) 305–316.
- [10] T. Wei and R. Klette: A wavelet-based algorithm for height from gradients. *Lecture Notes in Computer Science*, **1998** (2001) 84-90.
- [11] T. Wei and R. Klette: A New Algorithm for Gradient Field Integration. *Image and Vision Computing New Zealand (IVCNZ'2001)*, Dunedin, New Zealand. (2001)
- [12] Z. Wu and L. Li: A line-integration based method for depth recovery from surface normals, *Computer Vision, Graphics, and Image Processing*, **43** (1988) 53–66.